High-strain measurement using fiber Bragg grating sensors

Sotoudeh, V., Black, R., Costa, J., Faridian, F., Moslehi, B., et al.

V. Sotoudeh, R. J. Black, J. Costa, F. Faridian, B. Moslehi, L. Oblea, W. P. Roush, G. Wang, Q. H. Zuo, "High-strain measurement using fiber Bragg grating sensors," Proc. SPIE 8690, Industrial and Commercial Applications of Smart Structures Technologies 2013, 869005 (29 March 2013); doi: 10.1117/12.2009277

SPIE.

Event: SPIE Smart Structures and Materials + Nondestructive Evaluation and Health Monitoring, 2013, San Diego, California, United States

High Strain Measurement Using Fiber Bragg Grating Sensors

V. Sotoudeh[a], R. J. Black[a], J. Costa[a], F. Faridian[a], B. Moslehi[a], L. Oblea[a]
W. P. Roush[b], G. Wang[b*], Q. H. Zuo[b]
[a] Intelligent Fiber Optic Systems Corporation (IFOS), Santa Clara, CA, 95054
[b] Dept. of Mechanical and Aerospace Engineering, University of Alabama in Huntsville, Huntsville, AL, 35899

ABSTRACT

Fiber Bragg Grating-based (FBG) strain sensors have been widely used in engineering applications requiring small size, light weight, amenability to multiplexing, and very fast response times. State-of-the-art FBG interrogators are capable of measuring as low as sub micro strains and as high as 1% fiber strain in tension and higher still under compression. In this paper, we will discuss the development of an FBG based real-time instrumentation system to conduct highly dynamic strain measurements during an impact. A high-speed FBG interrogation system was used along with an FBG sensor data analysis software for efficient post-processing. In order to capture high strain data during an impact event, one needs to conduct measurements at very fast speeds and simultaneously to maintain FBG sensor survivability. A high strain FBG fixture was designed accordingly. Such high strain fixture allows the FBG strain sensor to measure the actual field strain with a reduction factor K in order to expand the strain measurement range. Numerical simulation results using finite element analysis (FEA) were used to validate the high strain fixture design analysis. Finally, a proof-of-concept FBG-based high strain measurement system has been demonstrated to measure dynamic strain data under impact tests. Experimental strain reduction factors were determined from the strain data and correlated well with FEA predicted values.

Keywords: FBG optical interrogator, Strain, K-factor, Final Element Analysis.

1. INTRODUCTION

Measurements of the whole-field surface deformation are very important in an impact event. Such information can help the designer to understand impact characteristics and improve the design of a structure or system used in the impact. Camera based metrology systems have been used to capture images during an impact. For ballistic impact applications where the velocity can be up to 300 m/s, however, it is still a serious challenge to meet the measurement requirements. Frame capture rates in excess of 1 million frames per second and several micron displacement resolutions must be achieved in order to capture the physical process taking place during the impact.

An optical fiber Bragg grating (FBG)-based real-time instrumentation system I*Sense® HS-48M developed by IFOS and capable of simultaneous multi-FBG sampling at up to 3 MS/s was used in this study to conduct quantitative evaluation of the whole-field dynamic response of ballistically impacted specimens. The sensing system is modular, electrically passive, electromagnetic interference (EMI) immune, and multiplexable (i.e., it can address at high-speeds many FBG sensors on a single lightweight commercial-grade optical fiber [1-4]). The key innovation is in the use of an advanced fiber optic sensing system with specialized strain fixtures to measure the spatial deformation of the object throughout the duration of the ballistic impact, which leads to the transient response and resulting deformation distribution measurements. In addition to providing significant extension of range and speed in dynamic strain measurements in extreme conditions, reductions in weight, power consumption and footprint, the solution can be applied to many applications involving high-rate events. Some examples are severe weather damage, puncture resistance, police protection, crashworthiness in vehicle designs and characterization of impact properties for applications ranging from composite structures such as lightweight shelters to sporting goods such as helmets.

The paper proceeds as follows. In section 2, we briefly discuss the FBG sensor system. This is followed by an FBG sensor fixture analysis, FEA simulation, and reduction factor validation in section 3. Section 4 presents the strain measurement results. A summary and some concluding remarks are given in section 5.

2. FBG SENSOR SYSTEM DESIGN

As shown schematically in Figure 1, a fiber Bragg grating [1-4] operates by acting as a wavelength selective filter that reflects a narrow band of light centered on the grating's characteristic wavelength referred to as the Bragg wavelength, λ_B. The Bragg wavelength is related to the grating pitch, Λ, and the mean refractive index of the core, n, by $\lambda_B = 2\Lambda n$.

* Corresponding Author, Email: Gang.Wang@uah.edu, Tel. 256-824-6209

Industrial and Commercial Applications of Smart Structures Technologies 2013,
edited by Kevin M. Farinholt, Steven F. Griffin, Proc. of SPIE Vol. 8690, 869005
 · doi: 10.1117/12.2009277

Both the fiber refractive index and the grating pitch vary when strain is applied to the FBG and/or the temperature is changed. Wavelength change measurement then provides a basis for strain and temperature sensing. For example, high-resolution strain sensing operation can be achieved by precise measurement of the wavelength [3-4].

FBGs have been established as a particularly important sensor component for static and dynamic strain measurements in smart structures. In many applications, arrays of FBG sensors along a single fiber at multiple locations are required to collect data samples at high speed with micro-strain resolution. Traditional approaches to processing the optical signals, however, either lack in sampling speed or are cost-prohibitive as the number of optical sensors increases. Recent advances in interrogation technology are opening up the possibility of supporting a large number of FBG sensors (on the order of a hundred per fiber) at high sampling speed (hundreds of kHz to MHz).

In order to meet the high-speed strain measurement requirements, IFOS modified its optical interrogator design to achieve the sampling rate of 500 kS/s simultaneously across a number of FBGs. In addition, a streamlining FBG sensor data analysis software tool was developed for efficiently post-processing. A FBG fixture strip with a set of strain reducing bridges and fiber adapters was used to conduct strain measurements as discussed in Section 4.

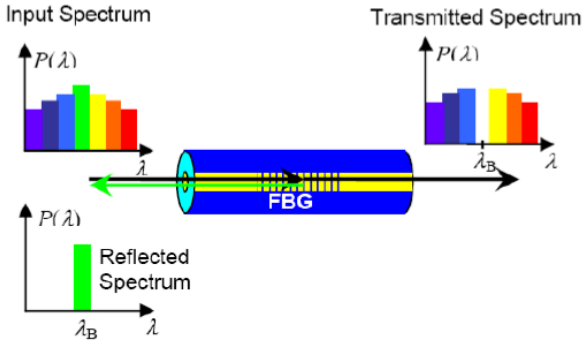

Figure 1: Functional principle of a fiber optic Bragg grating

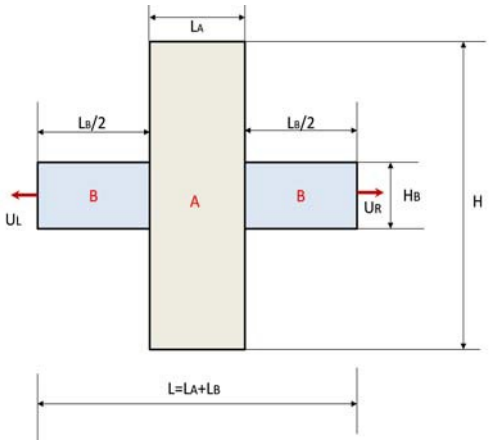

Figure 2: FBG Fixture

3. FBG FIXTURE DESIGN

Zhou *et al.* developed a simple analysis to study the sensitivity of strain measurement of FBGs [5]. We adopted their analysis to design our FBG fixture. Figure 2 shows a schematic of a FBG fixture. If the strain in the FBG section (section A) is denoted as ε_f and the strain in the side arm (section B) as ε_B, then the strain in the sensor is

$$\varepsilon_S = \frac{\Delta L}{L} = \frac{L_A\varepsilon_f + L_B\varepsilon_B}{L_A + L_B} = \frac{L_A}{L}\varepsilon_f + \left(1 - \frac{L_A}{L}\right)\varepsilon_B \tag{1}$$

where the variables are as defined in Figure 2. It should be noted that both sections A and B have a thickness which will be denoted t_A and t_B, respectively. Assuming the strain distributions in each section are uniform, the consideration of equilibrium of the sensor gives

$$E_A A_A \varepsilon_f = E_B A_B \varepsilon_B \tag{2}$$

Hence the strains in the FBG (section A) and in the side arm (section B) are related by

$$\varepsilon_B = \frac{E_A A_A}{E_B A_B}\varepsilon_f \tag{3}$$

The substitution of Eq. 3 into Eq. 1 yields the relationship between the sensor strain and the FBG strain

$$\varepsilon_S = \left(\frac{L_A}{L} + \left(1 - \frac{L_A}{L}\right)\frac{E_A A_A}{E_B A_B}\right)\varepsilon_f \tag{4}$$

Finally, using the sensor-to-FBG strain relationship, a reduction factor, K, can be calculated

$$K = \frac{\varepsilon_s}{\varepsilon_f} \tag{5}$$

$$K = \frac{L_A}{L} + \left(1 - \frac{L_A}{L}\right)\frac{E_A A_A}{E_B A_B} \tag{6}$$

The reduction factor K is the factor by which the strain in the sample is scaled down to the FBG fiber. Having a large reduction factor renders the loading environment much more favorable for the sensitive optical fibers used in FBG sensors, making the measurements of high strains in the impacted samples possible.

3.1 FEA Simulation

In order to validate the reduction factor predicted by Eq. 6, a finite element analysis (FEA) was conducted to calculate the strains in the fixture. The fixture was meshed using tetrahedron elements (tet10) and only half of the model was used due to symmetry. The FEA meshing of the fixture is shown in Figure 3. A prescribed displacement was applied to the sensor to simulate a specific strain input. Three cases were set up to simulate the strain levels of 0.01%, 0.10%, and 0.18%. It was assumed that the fixture is made of cold drawn steel, with the Young's modulus of 205 GPa and Poisson's ratio of 0.29. Figure 4 shows the contours of the strains in the fixture for an applied strain of 0.18%.

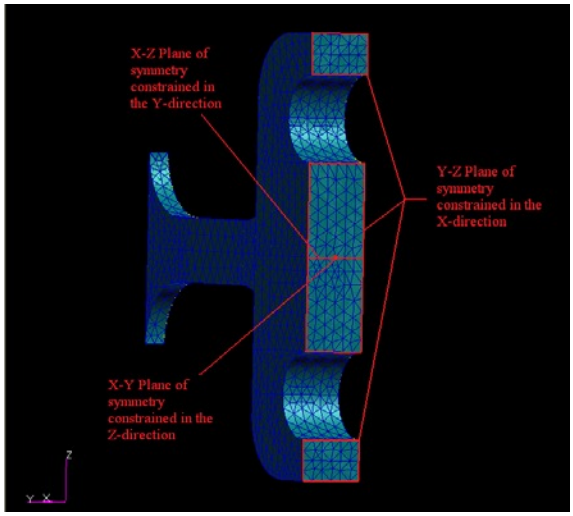

Figure 3 Meshed FBG model showing constraints

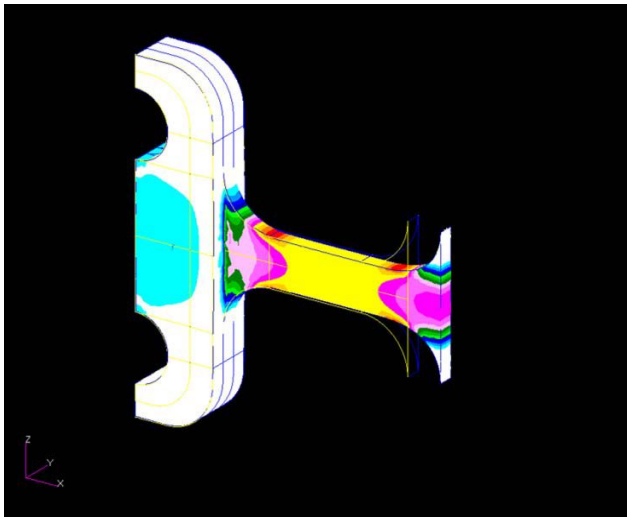

Figure 4: Strain contour results for 0.18% strain

Table 1: Sensor Dimensions

$\mathbf{L_A}$ [mm]	10.0
L [mm]	34.0
H [mm]	21.0
$\mathbf{H_B}$ [mm]	3.00
$\mathbf{t_A}$ [mm]	3.00
$\mathbf{t_B}$ [mm]	1.00

3.2 K-factor Result

Table 1 shows the dimension of the fixture structure. Using Eq. 6, a theoretical reduction value was found to be K_T = 15.1. We selected groups of nodes to calculate the average strains in each region from the FEA results. Table 2 shows a comparison of the strains in the FBG, predicted theoretically and the corresponding results from the FEA simulations. It

is seen that the theoretical values match reasonably well with the FEA results. Corresponding reduction factors were also determined from the FEA calculations and are shown in Table 3. These results of K_T = 14.4 to 14.5 compare favorably with the theoretical value of K_T = 15.1, indicating that the simple analytical model can be used to design a FBG fixture.

Table 2: Comparison of simulated and theoretical strains

Sensor Strain Case	0.01%	0.10%	0.18%
Average FEA FBG Strain [με]	6.92	69.5	125
Theoretical FBG Strain [με]	6.61	66.1	119

Table 3: Reduction value comparisons

Sensor Strain Case	0.01%	0.10%	0.18%
Calculated K	14.5	14.4	14.4

4. RESULTS

4.1 Fixture Fabrication

A single FBG fixture was fabricated, as shown in Figure 5. The final footprint of the sensor was 50 x 35 mm. In addition, a steel test plate was machined with four individual fixtures. The dimension of the plate was 24'' (length) by 4" (width) by 3/16" (thickness), as show in Figure 6.

Figure 5: Single manufactured FBG fixture

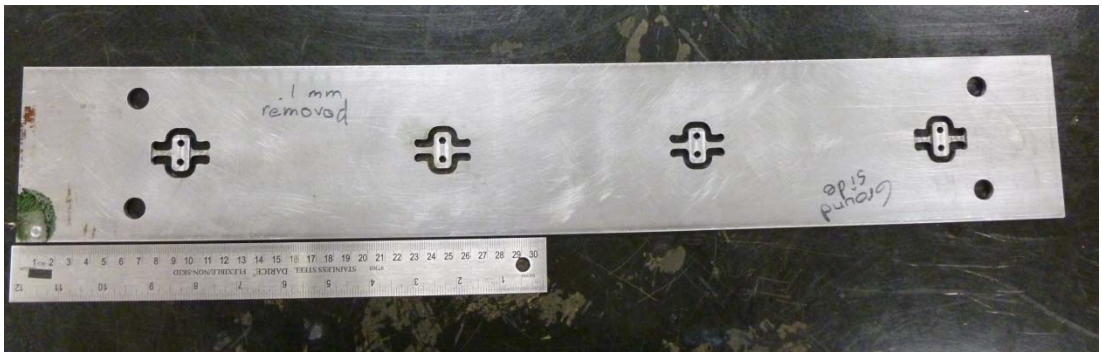

Figure 6: A plate (Labeled as Test Plate A) with four integrated FBG fixtures

It was shown through FEA analysis in section 3.2 that the theoretical equations used for predicting the strain reduction factor of a single fixture were validated. As shown in Figure 6, a plate (labeled as Test Plate A) with four integrated FBG fixtures was used in the ballistic tests. To determine the strain reduction factor for each fixture using FEA, similar to the discussion in Section 3, a simple static simulation was conducted. Each K-factor was calculated accordingly by determining the ratio between the average strain in the FBG section and the area

above the FBG fixture. The FEA mesh and strain contour plot are shown Figure 7 and Figure 8, respectively. The K-value was 4.81 for the high strain-reduction fixtures (located at both ends), and a K value of 3.05 was computed for the low strain-reduction fixtures (located at center).

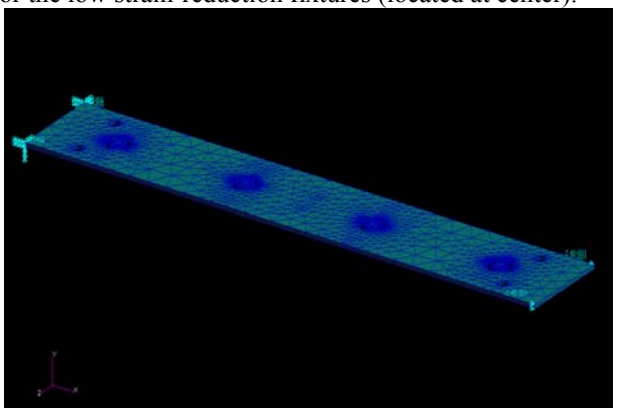

Figure 7: FEA mesh Test Plate A

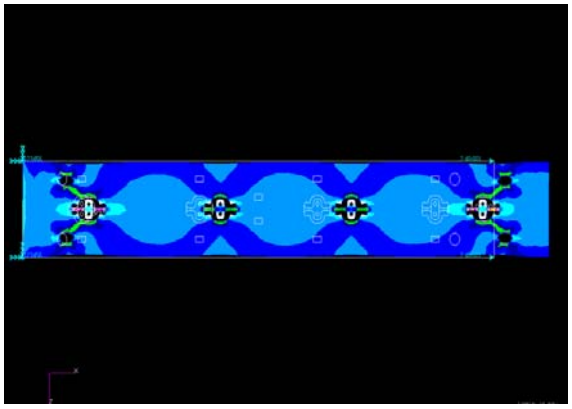

Figure 8: Strain contour for Test Plate A

4.2 Experimental Setup

The IFOS high speed FBG interrogation system was adapted to meet impact testing requirements. For the purposes of these tests, the system was run at 500 kS/s in conjunction with the strain reduction fixture. Prior to testing the FBG fixture, an investigation of a new fiber type developed by Corning was performed. The new fiber, ClearCurve ZBL, reduces bending loss and remains compatible with single mode fibers. Two standard reference fibers along with the ZBL fiber were attached to a steel plate using M-bond 200 and subjected to ballistic impact. After the test runs, the fibers were inspected for any damage. No damages were observed in any of the fibers, confirming that the new ZBL fiber would be an acceptable choice for FBG and ballistic tests. It was also confirmed that the interrogator system could simultaneous multi-FBG optical sensing at a much higher sampling rate compared to existing state of the art. The testing of the FBG fixture plate was accomplished by shooting at the middle of Test Plate A, using a blank air gun with different sizes of ballistic slugs. Figure 9 shows the sensor placement. Electrical strain gages and optical FBG sensors were mounted on the surface of the Test Plate A. All sensors were oriented to measure longitudinal strains. High K-value fixtures (with FEA prediction of 4.81) were placed at both ends. Low K-value fixtures (with FEA prediction of 3.05) were placed in the center region as shown in Figure 8.

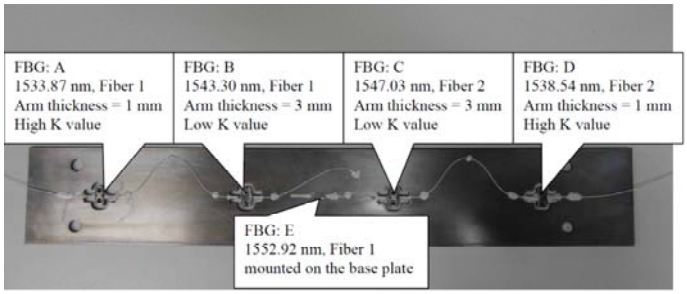

Figure 9: Test plate A with instrumented sensors

4.3 Impact Strain Results

We performed a series of air gun tests on the Test plate A (as shown in Figure 9) using the 3" slug under 90 psi air pressure. Figure 10 and Figure 11 show the first 100 milliseconds of strain measurements from both FBG sensors at 500 kHz sampling rate and strain gages. The following observations are made from the measurements:

- As shown in Figure 10, FBG at location E (middle of plate) measured a maximum tensile strain of 4000 με, while strain gages at the same location did not produce good data.
- There is a reasonable match between FBG-B and FBG-C measurements as expected since high strain fixtures at locations B and C are symmetrically located 3" from the slug hit point in the middle of the plate.
- Comparing FBG-A (Figure 11) and strain gage A readings, the high strain fixture at location A has a measured K factor of 5.5, based on the peak strain ratio of 2200/400. This is slightly higher than the predicted value of

4.81 from the Test Plate A's FEA static simulation as shown in Figure 8. A more detailed impulse response analysis for the Test Plate A is expected to further validate the reduction factor prediction.

- The difference in waveform obtained from FBG-A and the strain gage A is due to
  - Inherent higher bandwidth of the FBG sensor compared to a strain gage sensor
  - The dynamic effect of the high strain fixture structure
- There is a similarity between the FBG-A and FBG-D measurements. This is expected since high strain fixtures at locations A and D are symmetrically located 9" from the slug impact point in the middle of the plate.

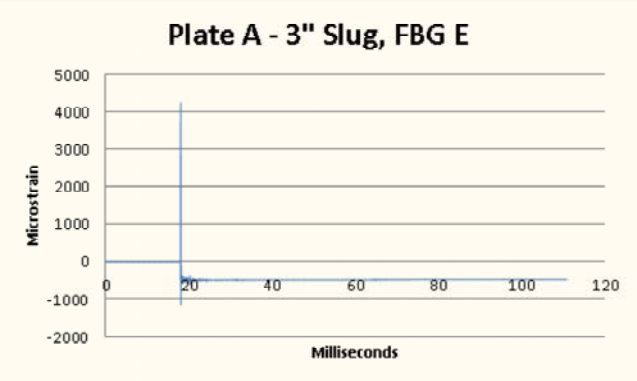

Figure 10: FBG sensor measurements at location E

5. CONCLUSION

We have successfully demonstrated the concept of an ultra-fast optical fiber Bragg grating (FBG)-based real-time instrumentation system for quantitative evaluation of the whole-field dynamic response of ballistically impacted specimens. A 500 kS/s FBG interrogator and a streamlining FBG sensor data analysis tool were developed in order to achieve efficient post-processing of data. In addition, we have carried out design, analysis, and fabrication of a high strain FBG fixture. Finally, impact tests were conducted and FBG strain sensors and strain gages were used to collect strain measurements. The FBG's higher bandwidth enables the capture of dynamic strain at very fast speeds. It is shown that the proposed high strain fixture provides an effective means of strain reduction and the system is capable of capturing fast dynamic strain data for the measurement of ballistic impacts.

6. ACKNOWLEDMENTS

This research was supported by the Army SBIR Phase I effort "Ballisitic Impact Assessment Systems", Contract No. W91CRB-12-C-0011, awarded to Intelligent Fiber Optic Systems Corporation (IFOS). Guidance and support from the technical point of contact Christopher Brewer and the Army research team at the Aberdeen Test Center is gratefully acknowledged.

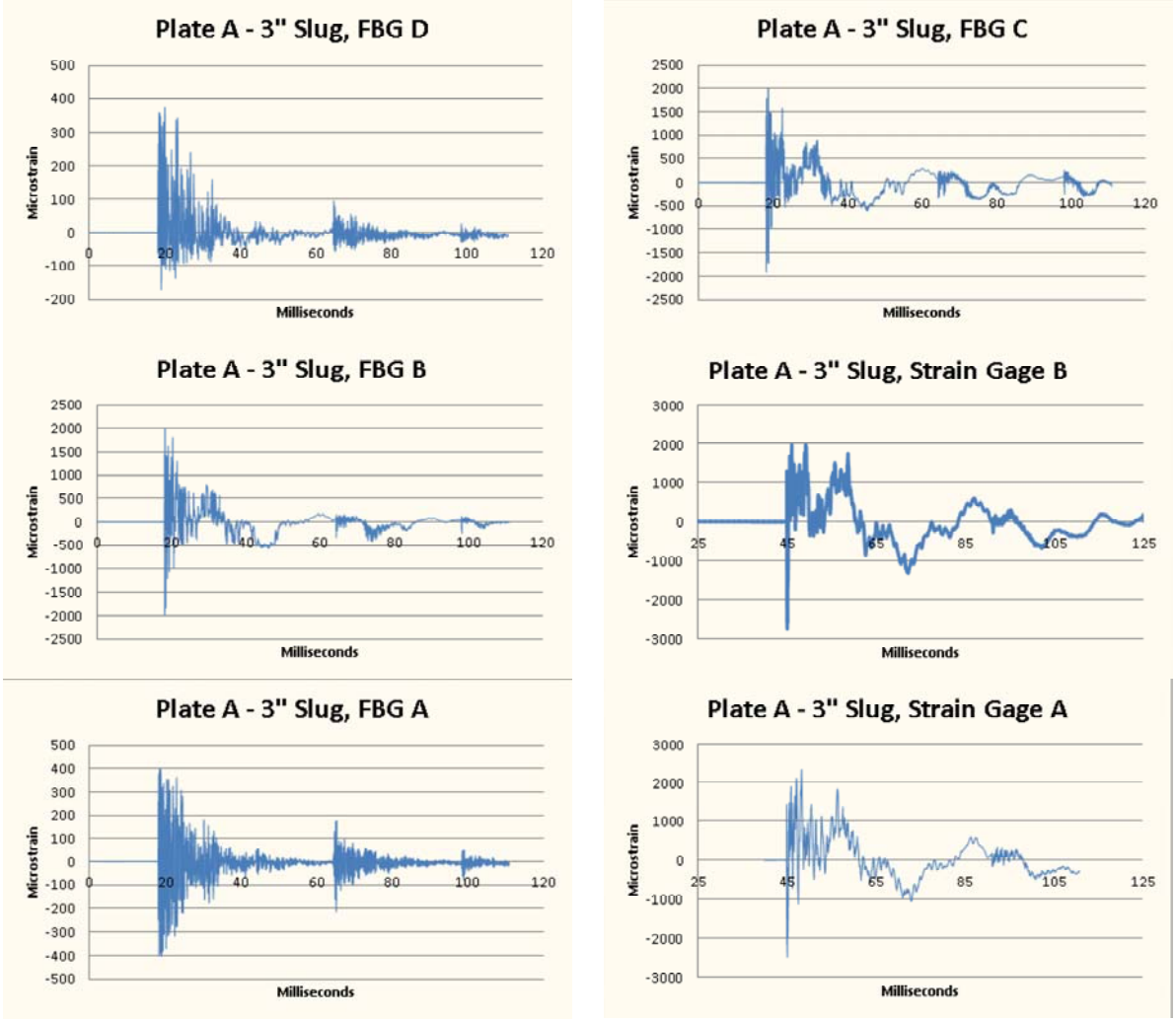

Figure 11: Time history data of strain measurements at location A-D

REFERENCES

[1] Grattan, K.T.V. and Meggitt, B.T., *Optical Fiber Sensor Technology: Fundamentals*, Kluwer Academic Publishers, Boston, 2000.

[2] Davis, M. A. and Kersey, A.D., "All-fiber Bragg grating strain-sensor demodulation technique using a wavelength division coupler," *Electronics Letters*, **30**, pp. 75-77, 1994.

[3] Black, R.J. and Moslehi, B., "Advanced end-to-end fiber optic sensing systems for demanding environments," (Invited Paper), *Proc. SPIE* **7817**, *SPIE Optics & Photonics, Conference OP413 Nanophotonics and Macrophotonics for Space Environments IV*, 2010.

[4] Moslehi, B., Black, R.J., Costa, J., Faridian, F. and Sotoudeh, V., "Highly Scalable Operational Sensor System for Harsh Environment Applications," *Proc. SAMPE* 2012, Baltimore.

[5] He, J. Zhou, Z., Dong, H.J., Zhang, G., "Study On a New Kind of Surface Sticking Strain Sensor With Sensitivity Enhanced Based on FBG," Proc. Of SPIE, Vol. 6595, 65953K, 2007.